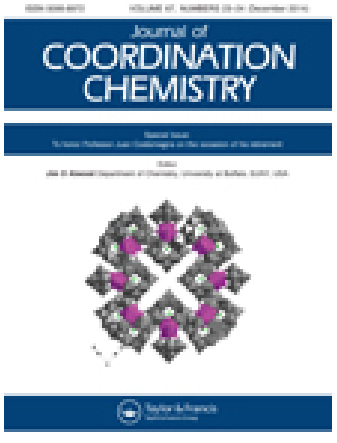

Journal of Coordination Chemistry
Publication details, including instructions for authors and subscription information:
http://www.tandfonline.com/loi/gcoo20

Macrocyclic Zn^{II} and Cu^{II} complexes as guests of the hybrid composites based on the layered $MnPS_3$ phase. Comparison of spectroscopic properties

Pablo Fuentealba[ab], Lorenzo Serón[ab], Camila Sánchez[ab], Jorge Manzur[bc], Verónica Paredes-Garcia[bd], Nancy Pizarro[d], Marjorie Cepeda[d], Diego Venegas-Yazigi[be] & Evgenia Spodine[ab]

[a] Facultad de Ciencias Químicas y Farmacéuticas, Universidad de Chile, Santiago, Chile

[b] CEDENNA, Santiago, Chile

[c] Facultad de Ciencias Físicas y Matemáticas, Universidad de Chile, Santiago, Chile

[d] Departamento de Ciencias Químicas, Universidad Andrés Bello, Santiago, Chile

[e] Facultad de Química y Biología, Universidad de Santiago de Chile, Santiago, Chile

Accepted author version posted online: 23 Sep 2014.Published online: 17 Oct 2014.

To cite this article: Pablo Fuentealba, Lorenzo Serón, Camila Sánchez, Jorge Manzur, Verónica Paredes-Garcia, Nancy Pizarro, Marjorie Cepeda, Diego Venegas-Yazigi & Evgenia Spodine (2014) Macrocyclic Zn^{II} and Cu^{II} complexes as guests of the hybrid composites based on the layered $MnPS_3$ phase. Comparison of spectroscopic properties, Journal of Coordination Chemistry, 67:23-24, 3894-3908, DOI: 10.1080/00958972.2014.968145

To link to this article: http://dx.doi.org/10.1080/00958972.2014.968145

Journal of Coordination Chemistry, 2014
Vol. 67, Nos. 23–24, 3894–3908, http://dx.doi.org/10.1080/00958972.2014.968145

Macrocyclic Zn^{II} and Cu^{II} complexes as guests of the hybrid composites based on the layered $MnPS_3$ phase. Comparison of spectroscopic properties

PABLO FUENTEALBA†‡, LORENZO SERÓN†‡, CAMILA SÁNCHEZ†‡, JORGE MANZUR‡§, VERÓNICA PAREDES-GARCIA‡¶, NANCY PIZARRO¶, MARJORIE CEPEDA¶, DIEGO VENEGAS-YAZIGI‡‖ and EVGENIA SPODINE*†‡

†Facultad de Ciencias Químicas y Farmacéuticas, Universidad de Chile, Santiago, Chile
‡CEDENNA, Santiago, Chile
§Facultad de Ciencias Físicas y Matemáticas, Universidad de Chile, Santiago, Chile
¶Departamento de Ciencias Químicas, Universidad Andrés Bello, Santiago, Chile
‖Facultad de Química y Biología, Universidad de Santiago de Chile, Santiago, Chile

(*Received 29 May 2014; accepted 29 August 2014*)

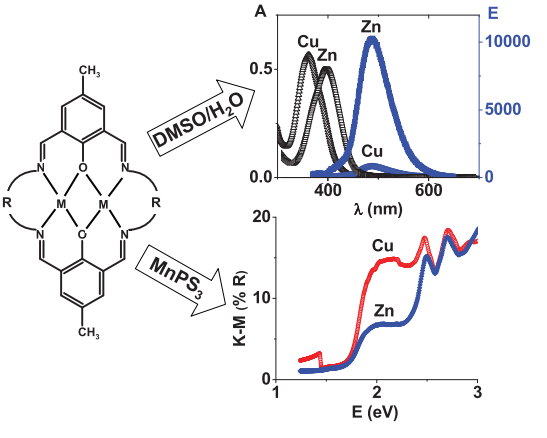

A family of macrocyclic complexes $[M_2L^nCl_2]$ have been synthesized and characterized (M: Cu^{II} or Zn^{II}; L^n: macrocyclic ligand derived from 2-hydroxy-5-methyl-1,3-benzenedicarbaldehyde and different aliphatic diamines and *o*-phenylenediamine). The influence of the aromaticity of the ligand and the metal center on the spectroscopic properties of the complexes (absorption and emission) has been studied. Making use of the weak interactions between hydrated potassium ions and the layers of the $K_{0.4}Mn_{0.8}PS_3$ precursor, the obtained macrocyclic complexes have been intercalated in the interlamellar space by a microwave assisted cationic exchange reaction. The optical properties of the obtained hybrid materials are reported. The absorption edge, recorded by solid state reflectance spectroscopy for Cu^{II} and the Zn^{II} macrocycle-based composites, is 1.67–1.76 eV, both shifted to lower energy compared with that of the pristine $MnPS_3$.

*Corresponding author. Email: espodine@uchile.cl
Dedicated to Professor Juan Costamagna.

Keywords: Macrocyclic complexes; $MnPS_3$ phase; Intercalation; Microwave radiation; Spectroscopic properties

1. Introduction

The study of materials with lamellar structure has generated interest due to their anisotropic physical properties and their structural conditions for becoming hosts of a wide range of inserted guest molecules by intercalation reactions, such as organic compounds [1], organometallic compounds [2], polymers [3, 4], monovalent and trivalent cations [1, 5–7]. The obtained hybrid materials have received attention mainly because the properties of the final composites are different from those of the initial precursors [1, 2, 4, 8–12].

Many layered compounds, such as double hydroxides [12–14], MS_2 (M = Ti, Mo, Nb, Ta) [15–18], and metal thiophosphates (MPS_3) [19, 20], have been reported. Among these, an important family of layered hosts is the transition metal MPS_3, where the Mn^{II} phase is one of the most interesting phases [21, 22]. The electric and magnetic properties for the $MnPS_3$ phase indicate a semiconductor character with low values of conductivity and a material presenting an antiferromagnetic exchange phenomenon [8]. From an optical point of view the $MnPS_3$ phase is almost a non-absorbing material. Furthermore, the intercalated $K_{0.4}Mn_{0.8}PS_3$ phase is a useful precursor, due to the existence of weak host-guest interactions between the interlamellar hydrated potassium ions and the layers of $MnPS_3$, which allow the exchange of these with bulky species, such as coordination compounds [22, 23]. The synthesis and structural characterization of macrocyclic complexes started forty years ago, as reported by Zanello *et al*. [24]; these complexes present different properties such as optical, magnetic, and antimicrobial activity that can modify the initial properties of $MnPS_3$ [25–28]. For example, most of the phenoxido-bridged macrocyclic dinuclear Cu^{II} complexes are known to present a strong antiferromagnetic interaction between the metal centers bridged by the phenoxido group [29]. By intercalating these macrocyclic complex species into the $MnPS_3$ phase, exhibiting the above-mentioned spectroscopic properties, it is possible to generate new composites with different physical properties due to the interaction of the host and guest moieties.

In the present work, a family of dinuclear Zn^{II} and Cu^{II} macrocyclic complexes have been synthesized. These complexes were intercalated in the $MnPS_3$ phase, by means of the $K_{0.4}Mn_{0.8}PS_3$ precursor, through a microwave assisted reaction. The layered materials have been characterized in order to investigate the influence of the Zn^{II} or Cu^{II} guest complex on the optical properties of the $MnPS_3$ layered host.

2. Experimental

2.1. *Characterization*

Copper and zinc analyses for the macrocyclic complexes were carried out on AAnalyst 700 Perkin Elmer equipment using an acetylene/air flame. The analyses of C, N, and H were done on a Thermo Fisher Flash 2000 Elemental Analyzer. FT-IR spectra were registered, using KBr pellets, on Bruker Vector 22 equipment. UV–vis absorption spectra were recorded on an Agilent 8453 Diode-Array spectrophotometer. The molar absorptivity, ϵ, was calculated from 10^{-7} to 10^{-4} M concentrations. Emission and excitation spectra were recorded on a Horiba Jobin-Yvon FluoroMax-4 spectrofluorometer with excitation wavelength 350 nm. The luminescent quantum yield was calculated using sulfate quinine in a

0.1 M solution of H_2SO_4 ($\Phi_{quinine} = 0.546$ [30]). The absorbance for the complexes and the reference compound were matched at 350 nm (values lower than 0.05 were employed). At this absorbance, the Cu^{II} complexes do not emit, while the Zn^{II} complexes present only one emission band.

X-ray powder diffraction was performed using a Bruker D-8 Advance diffractometer with a Cu Kα1 radiation in the $5° < 2\theta < 60°$ range. Scanning electron microscopy (SEM) was done using a Jeol Scanning Microscope (JSM-5410), with an Oxford Link Isis energy dispersive X-ray detector (EDXS). Diffuse reflectance spectra of solid samples were recorded on Perkin Elmer equipment (Lamba 1050 UV/vis/NIR Spectrometer).

2.2. *Syntheses*

All the solvents were distilled before use, while amines and inorganic salts were used as received. Pure elements were used to synthesize the host $MnPS_3$ phase using the synthetic method reported by Ruiz-León *et al.* [7]. The potassium precursor was synthesized by continuous stirring of the pristine phase in a 2 M potassium chloride solution for 24 h at room temperature [22]. The macrocyclic complexes were intercalated by a microwave assisted reaction (12 min. 800 W), as described by Spodine *et al.* [23]. The microwave apparatus for synthesis was a Millestone, model LAVIS 1000 Multi-Quant, with a frequency of 2.459 GHz.

The synthesis of all the complexes was based on 2-hydroxy-5-methyl-1,3-benzenedicarbaldehyde, which was synthesized by oxidation of 2,6-bis(hydroxymethyl)-*p*-cresol, by the procedure described by Papadopoulao *et al.* [31].

2.3. *Synthesis of 2-hydroxy-5-methyl-1,3-benzenedicarbaldehyde*

2,6-Bis(hydroxymethyl)-*p*-cresol (13.8 g) was dissolved in 1 L of chloroform under continuous stirring at room temperature. Manganese dioxide (120 g) was added slowly to the reaction mixture under continuous stirring, and the final suspension was refluxed for 6 h. The obtained mixture was cooled to room temperature and filtered. The yellow solution was evaporated under vacuum and the obtained yellow solid was purified by sublimation. The product was characterized by FTIR spectroscopy (KBr pellets): 3028–2924 (ν_{C-H} aromatic ring), 2872 (ν_{C-H} aldehyde), 1681, 1666 ($\nu_{C=O}$ aldehyde). Anal. Calcd ($C_9H_8O_3$) (%): C, 65.85; H, 4.91. Found (%): C, 64.5; H, 5.1.

2.4. *Syntheses of [2 + 1] hemicyclic ligands with aliphatic amines*

The hemicyclic ligand was obtained using the corresponding aliphatic amine. In 10 mL of 2-propanol 150 mg (0.914 mM) of 2-hydroxy-5-methyl-1,3-benzenedicarbaldehyde was dissolved with continuous stirring at room temperature. The appropriate aliphatic diamine (ethylenediamine (27 μL) (**I**), 1,3-diaminopropane (34 μL) (**II**), 1,3-diamino-2-propanol (37 mg) (**III**)) was added dropwise (90% of the corresponding molar relation, 0.411 mM), thus avoiding formation of the macrocyclic species, and left to react for one hour. The solutions were cooled to 5 °C, and the yellow–orange solids that precipitated were washed with 2-propanol and dried under vacuum (scheme 1).

(**I**) Yield; 100 mg, 62%. Anal. Calcd ($C_{20}H_{20}N_2O_4$): C 68.17; H, 5.72; N, 7.95. Found for (**I**) (%): C, 67.8; H, 6.2; N, 7.9.

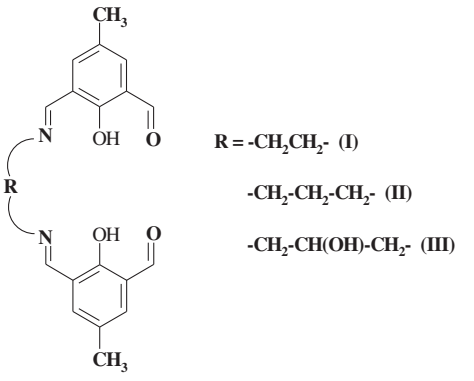

Scheme 1. Hemicyclic ligands.

(**II**) Yield; 80 mg, 47%. Anal. Calcd ($C_{21}H_{22}N_2O_4$): C 68.84; H, 6.05; N, 7.65. Found for (**II**) (%): C, 69.0; H, 6.3; N, 7.7.

(**III**) Yield; 80 mg, 45%. Anal. Calcd ($C_{21}H_{22}N_2O_5$): C 65.96; H, 5.80; N, 7.33. Found for (**III**) (%): C, 65.1; H, 6.0; N, 7.3.

The obtained FTIR spectra (KBr pellets) have the same pattern for all the hemicyclic ligands: 3030–2850 (ν_{C-H} aromatic ring and aliphatic chain from the amine), 1666 ($\nu_{C=O}$ aldehyde), 1640 ($\nu_{C=N}$ Schiff base), 1565 ($\nu_{C=C}$ aromatic ring).

2.5. *Syntheses of the macrocyclic complexes*

2.5.1. Homonuclear symmetric complexes. Symmetric homonuclear macrocyclic complexes were synthesized by a template reaction, similar to the procedure described by Paredes–García *et al.* [32]. 2-Hydroxy-5-methyl-1,3-benzenedicarbaldehyde (150 mg, 0.914 mM) was refluxed for 1.5 h with 125 mg of $ZnCl_2$ (or $CuCl_2$, 156 mg, 0.914 mM) in 2-propanol (25 mL) under a nitrogen atmosphere. Then 0.914 mM of the corresponding diamine (ethylenediamine (**1**,**5**) (55 mg), 1,3-diaminepropane (**2**,**6**) (68 mg), 1,3-diamine-2-propanol

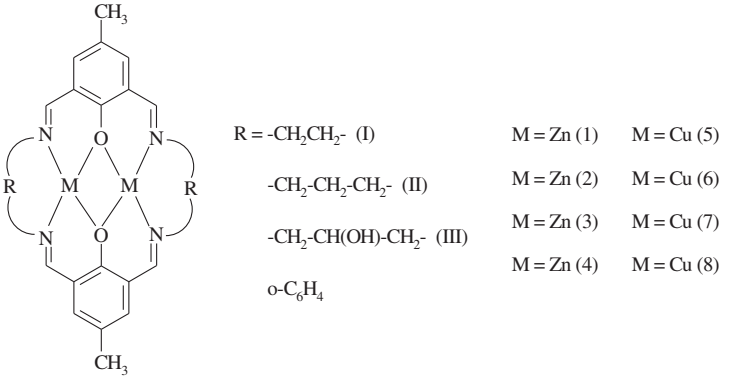

Scheme 2. Symmetric macrocyclic complexes (chloride ligands have been omitted for clarity).

(**3**,**7**) (82 mg) or *o*-phenylenediamine (**4**,**8**) (100 mg)) dissolved in 10 mL 2-propanol were added, and the reacting mixture was refluxed for 30 min, and left to react further at room temperature with stirring for 24 h. The obtained solids were washed with 2-propanol and methanol, and dried in vacuum (scheme 2).

$[Zn_2L^1Cl_2]$, $C_{22}H_{22}Cl_2N_4O_2Zn_2$ (**1**). Yield; 220 g, 84%. Anal. Calcd (%): C, 45.86; H, 3.85; N, 9.72; Zn, 22.70. Found (%): C, 45.1; H, 3.9; N, 9.8; Zn, 22.2.

$[Zn_2L^2Cl_2]$, $C_{24}H_{26}Cl_2N_4O_2Zn_2$ (**2**). Yield; 225 mg, 81%. Anal. Calcd (%): C, 47.71; H, 4.34; N, 9.27; Zn, 21.70. Found (%): C, 47.9; H, 4.4; N, 9.2; Zn, 21.0.

$[Zn_2L^3Cl_2]$, $C_{24}H_{26}Cl_2N_4O_4Zn_2$ (**3**). Yield; 240 mg, 83%. Anal. Calcd (%): C, 45.31; H, 4.12; N, 8.81; Zn, 20.56. Found (%): C, 45.4; H, 4.1; N, 8.7; Zn, 20.8.

$[Zn_2L^4Cl_2]$, $C_{30}H_{22}Cl_2N_4O_2Zn_2$ (**4**). Yield; 230 mg, 75%. Anal. Calcd (%): C, 53.60; H, 3.30; N, 8.33; Zn, 19.46. Found (%): C, 53.3; H, 3.4; N, 8.4; Zn, 19.3.

$[Cu_2L^1Cl_2](H_2O)_2$, $C_{22}H_{26}Cl_2N_4O_4Cu_2$ (**5**). Yield; 220 mg, 79%. Anal. Calcd (%): C, 43.43; H, 4.31; N, 9.21; Cu, 20.89. Found (%): C, 43.3; H, 4.3; N, 9.3; Cu, 20.8.

$[Cu_2L^2Cl_2](H_2O)_2$, $C_{24}H_{30}Cl_2N_4O_4Cu_2$ (**6**). Yield; 225 mg, 78%. Anal. Calcd (%): C, 45.29; H, 4.75; N, 8.80; Cu, 19.97. Found (%): C, 45.1; H, 4.8; N, 8.9; Cu, 20.3.

$[Cu_2L^3Cl_2](H_2O)_2$, $C_{24}H_{30}Cl_2N_4O_6Cu_2$ (**7**). Yield; 230 mg, 76%. Anal. Calcd (%): C, 43.12; H, 4.52; N, 8.38; Cu, 19.01. Found (%): C, 43.3; H, 4.6; N, 8.2; Cu, 18.9.

$[Cu_2L^4Cl_2](H_2O)_2$, $C_{30}H_{26}Cl_2N_4O_4Cu_2$ (**8**). Yield; 220 mg, 68%. Anal. Calcd (%): C, 51.14, H, 3.72; N, 7.95; Cu, 18.04. Found (%): C, 51.3; H, 3.8; N, 7.8; Cu, 18.0.

The FTIR spectra (KBr pellets) of all symmetric macrocyclic complexes show three main vibration bands at 3030–2850 (ν_{C-H} aromatic ring and aliphatic chain from the amine); 1640 ($\nu_{C=N}$ Schiff base); 1565 cm^{-1} ($\nu_{C=C}$ aromatic ring). Furthermore, a band typical of the ortho aromatic substitution is observed at 760 cm^{-1}.

2.5.2. Homonuclear unsymmetric complexes. This family of macrocyclic species was obtained through a stepwise reaction by a procedure similar to that reported by Sreedaran *et al*. [33]. The procedure can be summarized as follows: to 0.273 mmoles of the corresponding hemicyclic ligand (**I**, 96 mg; **II**, 100 mg; or **III**, 104 mg) suspended in 2-propanol, triethylamine (80 μL) was added to deprotonate the ligand. A solution of the metallic salt (0.545 mM, 75 mg $ZnCl_2$, or 93 mg of $CuCl_2{\cdot}2H_2O$) in 10 mL of 2-propanol was added dropwise and the mixture was reacted for one hour. Finally, *o*-phenylenediamine (0.273 mM, 30 mg) was added and the reaction mixture was stirred at room temperature for 24 h. The solid was filtered off, washed with 2-propanol and methanol, and dried (scheme 3).

$[Zn_2L^5Cl_2]$, $C_{26}H_{22}Cl_2N_4O_2Zn_2$ (**9**). Yield; 145 mg, 85%. Anal. Calcd (%): C, 50.03; H, 3.55; N, 8.98; Zn, 20.95. Found (%): C, 50.2; H, 3.6; N, 8.8; Zn, 20.5.

$[Zn_2L^6Cl_2]$, $C_{27}H_{24}Cl_2N_4O_2Zn_2$ (**10**). Yield; 128 mg, 74%. Anal. Calcd (%): C, 50.81; H, 3.79; N, 8.78; Zn, 20.49. Found (%): C, 50.9; H, 3.7; N, 8.9; Zn, 20.6.

$[Zn_2L^7Cl_2]$, $C_{27}H_{24}Cl_2N_4O_3Zn_2$ (**11**). Yield; 133 mg, 75%. Anal. Calcd (%): C, 49.57; H, 3.70; N, 8.56; Zn, 19.99. Found (%): C, 49.4; H, 3.7; N, 8.6; Zn, 19.8.

$[Cu_2L^5Cl_2](H_2O)_2$, $C_{26}H_{26}Cl_2N_4O_4Cu_2$ (**12**). Yield; 156 mg, 87%. Anal. Calcd (%): C, 47.57; H, 2.99; N, 8.53; Cu, 19.36. Found (%): C, 47.9; H, 4.1; N, 8.4; Cu, 18.9.

$[Cu_2L^6Cl_2](H_2O)_2$, $C_{27}H_{28}Cl_2N_4O_4Cu_2$ (**13**). Yield; 114 mg, 62%. Anal. Calcd (%): C, 48.36; H, 4.21; N, 8.36; Cu, 18.95. Found (%): C, 48.2; H, 4.2; N, 8.4; Cu, 19.0.

$[Cu_2L^7Cl_2](H_2O)_2$, $C_{27}H_{28}Cl_2N_4O_5Cu_2$ (**14**). Yield; 137 mg, 74%. Anal. Calcd (%): C, 47.24; H, 4.11; N, 8.16; Cu, 18.51. Found (%): C, 46.7; H, 4.0; N, 8.0; Cu, 18.4.

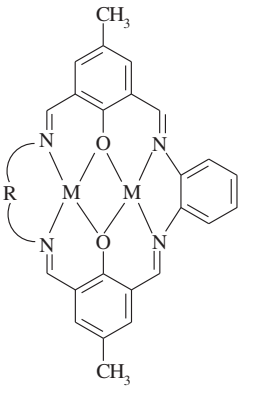

R = -CH_2CH_2- M = Zn (9) M = Cu (12)

-CH_2-CH_2-CH_2- M = Zn (10) M = Cu (13)

-CH_2-CH(OH)-CH_2- M = Zn (11) M = Cu (14)

Scheme 3. Unsymmetric macrocyclic complexes (chloride ligands have been omitted for clarity).

As for the unsymmetric macrocyclic complexes described above, the FTIR spectra for the unsymmetric macrocyclic complexes show a similar pattern: 3030–2850 cm^{-1} (ν_{C-H}), 1640 cm^{-1} ($\nu_{C=N}$), 1565 cm^{-1} ($\nu_{C=C}$). In addition, the band typical of the ortho aromatic substitution is observed at 760 cm^{-1}.

2.6. *Synthesis of the pristine phase, $MnPS_3$, and the potassium precursor $K_{0.4}Mn_{0.8}PS_3$*

Pure $MnPS_3$ phase was synthesized using the ceramic method, as described in the literature [7]. High purity elements (Mn, P, S) were mixed in a 1 : 1 : 3 molar ratio and reacted in an evacuated quartz tube at 750 °C for seven days. Then, the reactor was slowly cooled and a green polycrystalline phase of Mn^{II} was obtained.

The potassium precursor was synthesized by stirring for 24 h at room temperature, a suspension of the solid phase $MnPS_3$, with an aqueous 2 M KCl solution [22]. The obtained light green potassium precursor was characterized by SEM-EDX giving a $K_{0.4}Mn_{0.8}PS_3$ stoichiometry.

2.7. *Microwave assisted exchange reaction of the interlamellar potassium ions by the macrocyclic complexes*

The potassium precursor, $K_{0.4}Mn_{0.8}PS_3$ (150 mg), was suspended in 15 mL of a concentrated methanolic solution of 0.16 mmoles of the corresponding macrocyclic complex. The suspension was irradiated with microwave radiation (800 W) for 12 min. The solid was filtered, washed with ethanol, followed by DMF, until the solvent became colorless. A representative series of complexes was intercalated: symmetric homonuclear Cu^{II} complexes derived from the aliphatic amines ethylenediamine and 1,3-diamino-2-propanol, $[Cu_2L^1]$ and $[Cu_2L^3]$; unsymmetric homonuclear Cu^{II} derived from the aliphatic amines ethylenediamine and 1,3-diamino-2-propanol and *o*-phenylenediamine $[Cu_2L^5]$ and $[Cu_2L^7]$; symmetric homonuclear Zn^{II} derived from ethylenediamine $[Zn_2L^1]$ and from *o*-phenylenediamine $[Zn_2L^4]$. The obtained composites were characterized by SEM-EDX giving the following stoichiometries: $[Cu_2L^1]_{0.07}K_{0.26}Mn_{0.8}PS_3$ ***(a)***, $[Cu_2L^3]_{0.07}K_{0.26}Mn_{0.8}PS_3$ ***(b)***, $[Cu_2L^5]_{0.08}K_{0.24}Mn_{0.8}PS_3$ ***(c)***, and $[Cu_2L^7]_{0.09}K_{0.22}Mn_{0.8}PS_3$ ***(d)***, for the Cu^{II} complexes, and $[Zn_2L^1]_{0.07}K_{0.26}Mn_{0.8}PS_3$ ***(e)***, $[Zn_2L^4]_{0.12}K_{0.16}Mn_{0.8}PS_3$ ***(f)*** for the Zn^{II} complexes.

3. Results and discussion

3.1. *Synthesis and structure*

The obtained Zn^{II} and Cu^{II} macrocyclic complexes were all characterized by elemental analyses and infrared spectra. The first coordination sphere of the Cu^{II} centers of the synthesized complexes was assumed to be five-coordinate, as determined by X-ray diffraction for **5**, **6**, **7**, and **8** in previous work [34–39]. The structure of **7** shows that the chlorides occupy axial positions in the first coordination sphere and are *trans* to each other [37], while the other reported complexes have oxygen donors in the axial positions, provided by water, methanol, DMF, nitrate or perchlorate [34–36, 38, 39]. Furthermore, analyses for the synthesized complexes are consistent with two solvation waters in the proposed structure of all the Cu^{II} complexes. In contrast, the elemental analyses for the Zn^{II} complexes are in agreement with an anhydrous structure, as was previously reported by Korupoju *et al.* for a similar macrocyclic complex [40]. These authors describe the first coordination sphere of the Zn^{II} chloride complex as being five-coordinate with a square base pyramidal geometry. Thus, both Cu^{II} and Zn^{II} series of complexes are assumed as having five-coordinate metal centers.

The combination of these molecular guests with layered hosts, such as $MnPS_3$, gives new functional materials. This can be accomplished by ion exchange reaction, which allows the organized assembly of molecules into the interlamellar space of layered frameworks. However, this synthetic procedure is time consuming, since the guest substitution is limited by diffusion processes, and the charge and size of the intercalated molecules. Therefore, the possibility to use microwave assisted intercalation has resulted in a promising synthetic alternative to obtain new hybrid materials, such as the composites reported in this work [23]. The microwave assisted synthesis permitted isolation and characterization of the following homonuclear-based composites: $[Cu_2L^1]_{0.07}K_{0.26}$ $Mn_{0.8}PS_3$ ***(a)***, $[Cu_2L^3]_{0.08}K_{0.26}$ $Mn_{0.8}PS_3$ ***(b)***, $[Cu_2L^5]_{0.08}K_{0.24}$ $Mn_{0.8}PS_3$ ***(c)***, $[Cu_2L^7]_{0.09}K_{0.22}Mn_{0.8}PS_3$ ***(d)***; $[Zn_2L^1]_{0.07}K_{0.26}Mn_{0.8}PS_3$ ***(e)***, $[Zn_2L^4]_{0.12}K_{0.16}Mn_{0.8}PS_3$ ***(f)***. These composites can also be obtained by the more classical ion exchange procedure, which involves stirring the suspension of $K_{0.4}Mn_{0.8}PS_3$ in a saturated solution of the corresponding macrocyclic complex for several weeks at room temperature. The materials resulting from the microwave assisted intercalation exhibit similar optical properties as the composites prepared by the classical ion-exchange route. Therefore, only the optical properties of the composites obtained by the microwave assisted method will be discussed in this work.

3.2. *Spectroscopic properties of the macrocyclic complexes*

All complex solutions were prepared in DMSO/H_2O mixtures (ratio 1 : 2). The absorption spectra were recorded from 300 to 800 nm, while the emission spectra were between 370 and 650 nm [27]. Both absorption and emission spectra will be analyzed and discussed.

The absorption and emission spectra for all complexes under study are shown in figures 1 and 2. Tables 1 and 2 summarize the results of the spectroscopic studies of homonuclear symmetric and unsymmetric complexes, respectively.

The absorption maxima did not change their position in the studied concentration range, so it was possible to infer that only one species was present in solution.

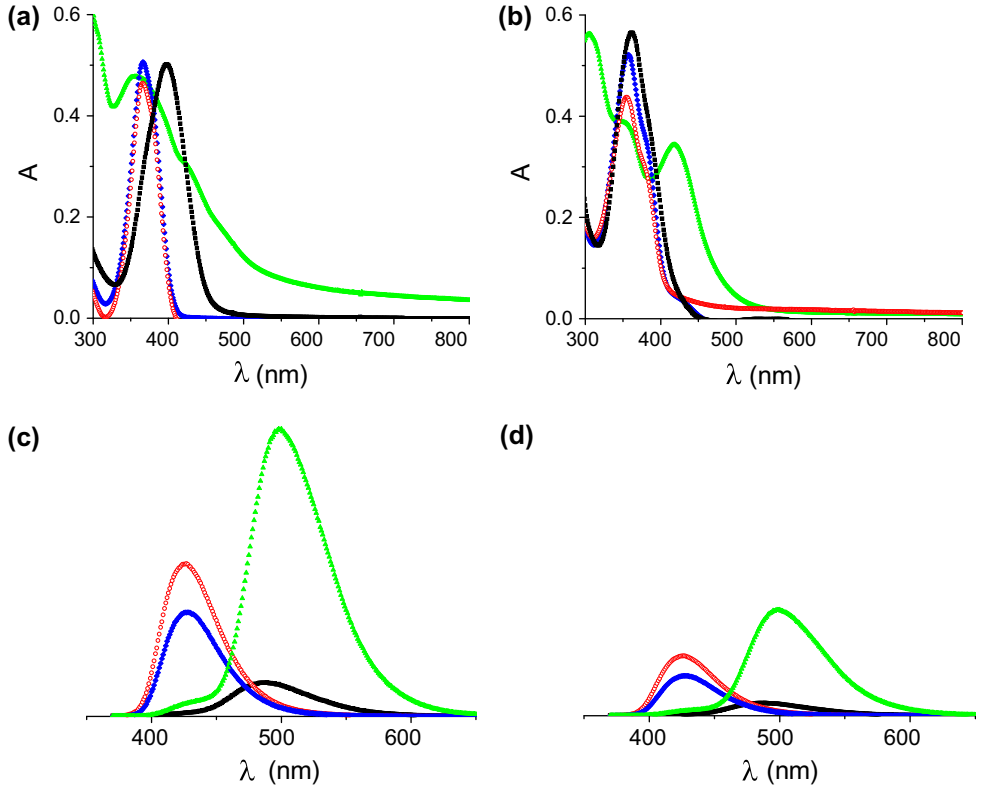

Figure 1. Absorption (a) and emission (c) spectra of the symmetric Zn^{II} complexes: (**1**) ■ black; (**2**) ○ red; (**3**) ♦ blue; (**4**) ▲ green. Absorption (b) and emission (d) spectra of the symmetric Cu^{II} complexes: (**5**) ■ black; (**6**) ○ red; (**7**) ♦ blue; (**8**) ▲ green (see http://dx.doi.org/10.1080/00958972.2014.968145 for color version).

3.2.1. Absorption spectra of Zn^{II} macrocyclic complexes. Zn^{II} symmetric complexes **1**, **2**, and **3** with macrocyclic ligands derived from aliphatic amines have only one absorption in the 370–400 nm range, while **4** with the macrocyclic ligand derived from *o*-phenylenediamine has two absorptions at 370 and 425 nm [figure 1(a)]. The absorption maxima are at 400 ($\varepsilon = 1.0 \cdot 10^4$ M^{-1} cm^{-1}) for **1**, 370 ($\varepsilon = 1.1 \cdot 10^4$ M^{-1} cm^{-1}) for **2**, 370 ($\varepsilon = 1.3 \cdot 10^4$ M^{-1} cm^{-1}) for **3**, and 370 and 425 nm ($\varepsilon = 1.5 \cdot 10^4$ and $8.8 \cdot 10^3$ M^{-1} cm^{-1}) for **4**. The higher energy band is associated with the $n \rightarrow \pi^*$ ligand-centered transition and the 425 nm maximum is assigned to a metal to ligand charge transfer band (MLCT) [41].

The unsymmetric Zn^{II} complex (**9**) shows a band at 370 nm ($\varepsilon = 6.9 \cdot 10^3$ M^{-1} cm^{-1}), with a small shoulder at 395 nm. The band at 370 nm is associated with a ligand-centered $n - \pi^*$ transition similar to the one of the symmetric complex, while the shoulder at 395 nm is ascribed to a MLCT absorption related to the *o*- phenylenediamine moiety of the ligand [32]. For the unsymmetric complexes (**10** and **11**) ligand-centered transition bands are observed at 350 nm ($\varepsilon = 8.6 \times 10^3$ (**10**); $\varepsilon = 1.1 \times 10^4$ M^{-1} cm^{-1} (**11**)) and the MLCT absorptions at 385 nm ($\varepsilon = 1.2 \times 10^4$ (**10**)) and 395 nm ($\varepsilon = 1.6 \times 10^4$ M^{-1} cm^{-1} (**11**)).

Due to the lower aromaticity of the unsymmetric ligands, the MLCT band is blue-shifted, as compared with the symmetric **4** derived from *o*-phenylenediamine. In addition, as shown

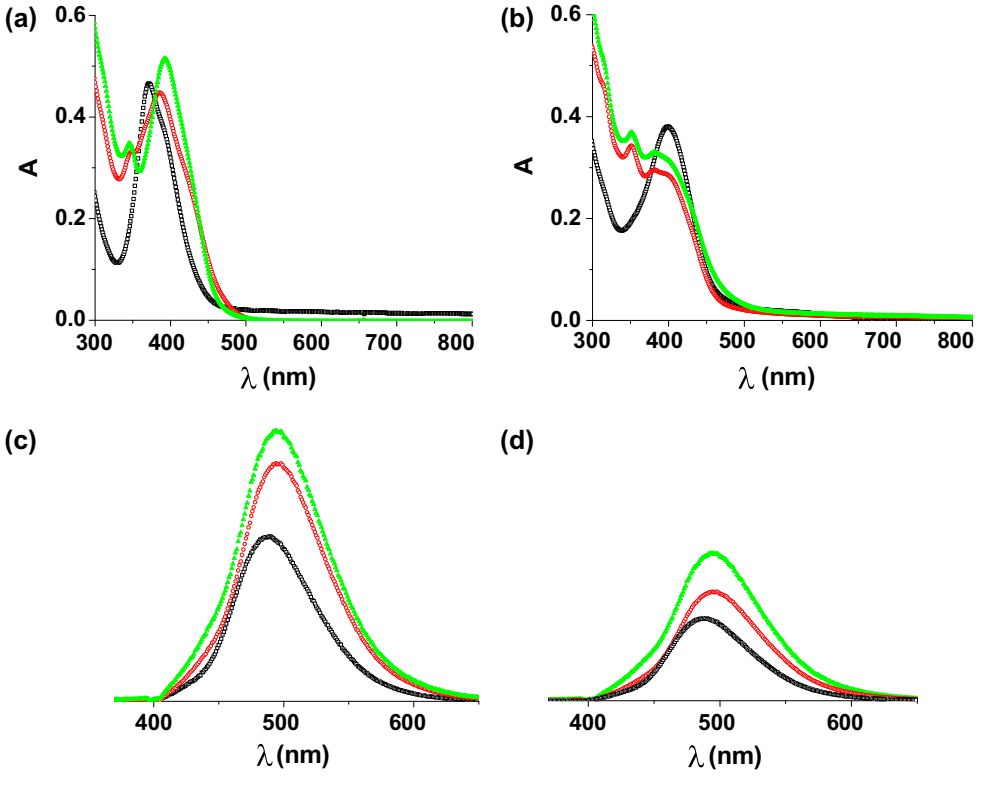

Figure 2. Absorption (a) and emission (c) spectra of the unsymmetric Zn^{II} complexes: (**9**) □ black; (**10**) ○ red; (**11**) ▲ green. Absorption (b) and emission (d) spectra of the unsymmetric Cu^{II} complexes: (**12**) □ black; (**13**) ○ red; (**14**) ▲ green (see http://dx.doi.org/10.1080/00958972.2014.968145 for color version).

Table 1. Spectroscopic data for the symmetric macrocyclic complexes.

Complex	N°	λ_{Abs} (nm)	ϵ (M^{-1} cm^{-1})	λ_{em} (nm)	ϕ (%)
$[Zn_2L^1]^{2+}$	(**1**)	400	1.0×10^4	487	3.0
$[Zn_2L^2]^{2+}$	(**2**)	370	1.1×10^4	427	5.6
$[Zn_2L^3]^{2+}$	(**3**)	370	1.3×10^4	427	6.9
$[Zn_2L^4]^{2+}$	(**4**)	370	1.5×10^4	500	14.3
		425	8.8×10^3		
$[Cu_2L^1]^{2+}$	(**5**)	360	5.7×10^3	487	–
		370	sh		
		550–700	$\sim 10^2$		
$[Cu_2L^2]^{2+}$	(**6**)	360	7.3×10^3	427	–
		370	sh		
		550–700	$\sim 10^2$		
$[Cu_2L^3]^{2+}$	(**7**)	360	6.6×10^3	427	–
		370	sh		
		550–700	$\sim 10^2$		
$[Cu_2L^4]^{2+}$	(**8**)	355	1.2×10^4	500	–
		418	1.1×10^4		
		550–700	$\sim 10^2$		

Table 2. Spectroscopic data for the unsymmetric macrocyclic complexes.

Complex	N°	λ_{Abs} (nm)	ϵ (M^{-1} cm^{-1})	λ_{em} (nm)	ϕ (%)
$[Zn_2L^5]^{2+}$	(**9**)	370	6.9×10^3	493	5.5
		395	sh		
$[Zn_2L^6]^{2+}$	(**10**)	350	8.6×10^3	496	7.8
		385	1.2×10^4		
$[Zn_2L^7]^{2+}$	(**11**)	350	1.1×10^4	496	8.4
		395	1.6×10^4		
$[Cu_2L^5]^{2+}$	(**12**)	370	sh	493	–
		400	1.1×10^4		
		550–700	$\sim 10^2$		
$[Cu_2L^6]^{2+}$	(**13**)	350	1.3×10^4	496	–
		390	1.1×10^4		
		550–700	$\sim 10^2$		
$[Cu_2L^7]^{2+}$	(**14**)	352	1.2×10^4	496	–
		385	1.1×10^4		
		550–700	$\sim 10^2$		

for the symmetric complexes, the intra-ligand bands in the complexes with 1,3-diaminepropane and 1,3-diamine-2-propanol (**2** and **3**) are blue-shifted compared to the macrocyclic ligand derived from ethylenediamine (**1**). Therefore, two maxima in the spectra of **10** and **11** can be distinguished.

3.2.2. Absorption spectra of Cu^{II} macrocyclic complexes. The Cu^{II} complexes derived from macrocyclic ligands with aliphatic amines (**5**, **6**, and **7**) present an unsymmetric band at 360 nm ($\epsilon = 5.7 \times 10^3$ (**5**); $\epsilon = 7.3 \times 10^3$ (**6**); $\epsilon = 6.6 \times 10^3$ M^{-1} cm^{-1} (**7**)), with a shoulder at 370–380 nm. The asymmetry of this absorption is assigned to the superposition of the phenolate to copper(II) charge transfer band that can be expected for phenoxido-Cu^{II} complexes in this same region [42]. Complex **8** has a band at 355 nm ($\epsilon = 1.2 \times 10^4$ M^{-1} cm^{-1}) and a second one at 418 nm ($\epsilon = 1.1 \times 10^4$ M^{-1} cm^{-1}). The band at higher energy is assigned to a ligand-centered $n \rightarrow \pi^*$ transition, as in the Zn^{II} complexes [figure 1(b)].

The unsymmetric complexes with Cu^{II} centers show spectra with two absorptions, as observed for spectra of the Zn^{II} ones (figure 2). Complex **12**, derived from ethylenediamine and *o*-phenylenediamine, shows an unsymmetric band at 400 nm ($\epsilon = 1.1 \times 10^4$ M^{-1} cm^{-1}) with a shoulder at 370 nm. These two absorption bands are assigned to the same transitions as in the Zn^{II} complex (**9**), derived from the same ligand. For the unsymmetric **13** and **14**, with 1,3-diaminepropane and 1,3-diamine-2-propanol moieties, a higher energy band at 350 and 352 nm ($\epsilon = 1.3 \times 10^4$ (**13**); $\epsilon = 1.2 \times 10^4$ M^{-1} cm^{-1} (**14**)) is observed, respectively. A second band is found at 390 and 385 nm ($\epsilon = 1.1 \times 10^4$ M^{-1} cm^{-1} (**13**); $\epsilon = 1.1 \times 10^4$ M^{-1} cm^{-1} (**14**)) for both complexes. These two absorptions have the same origin as in **12**, where the ligand-centered $n - \pi^*$ transition is shifted to higher energies in comparison to complexes with ethylenediamine.

All spectra of the Cu^{II} complexes are characterized by a weak band at 550–700 nm ($\epsilon = \sim 10^2$ M^{-1} cm^{-1}) ascribed to d–d transition of the copper ion.

3.2.3. Emission spectra of Zn^{II} macrocyclic complexes. Figure 1(c) shows the corresponding spectra of the symmetric Zn^{II} complexes, which emit at 487 (**1**), 427 (**2**), 427 (**3**),

and 500 nm (**4**). The calculated percentages of the quantum yield were 3.0 (**1**), 5.6 (**2**), 6.9 (**3**), and 14.3% (**4**).

As can be observed, the emission band for the complex with the aromatic ligand (**4**) is red-shifted compared to symmetric complexes with macrocyclic ligands based on non-aromatic amines (**1**, **2**, and **3**). Macrocyclic **1** showed the lowest quantum yield, being doubled when the aliphatic chain increased by one carbon in **2** and **3** (table 1). The presence of the OH substituent in the aliphatic amine of the macrocyclic ligand of **3** did not affect the emission wavelength of the corresponding complex, as compared with **2**, while the quantum yield showed a slight increase. Complex **4**, whose ligand is completely delocalized, shows the highest quantum yield.

Figure 2(c) shows the corresponding emission spectra of the unsymmetric Zn^{II} complexes. Complex **9** whose ligand is derived from ethylenediamine and *o*-phenylenediamine shows an emission band at 493 nm (ϕ, 5.5%). A comparison of the spectra indicates that the unsymmetric **9** emits at a wavelength between the emissions of **1** and **4**, corresponding to the symmetric macrocyclic complexes derived from ethylenediamine and *o*-phenylenediamine, respectively (figure 3). Similar behavior is observed for the unsymmetric macrocyclic **10** (ϕ, 7.8%) and **11** (ϕ, 8.4%); they emit between the emission wavelengths of the corresponding symmetric complex with the aliphatic amine (**2**) and the symmetric complex with *o*-phenylenediamine (**4**).

3.2.4. Emission spectra of Cu^{II} macrocyclic complexes. The Cu^{II} macrocyclic complexes did not emit under the conditions for the Zn^{II} complexes. However, when the concentration of the complexes was increased and the equipment setup was modified, the emission band could be detected. Quantum yields could not be measured for these complexes. Symmetric and unsymmetric Cu^{II} species have the same emission behavior as the Zn^{II} symmetric (figure 1) and unsymmetric (figure 2) complexes. Among the Cu^{II} macrocyclic complexes, the complex with the aromatic amine (**8**) presents the most intense band, as compared with the symmetric complexes with aliphatic amines and the unsymmetric complexes.

Considering that both Zn^{II} and Cu^{II} complexes with the same macrocyclic ligand emit at the same wavelength, as shown in tables 1 and 2, it is possible to infer that the emission proceeds via an intraligand process. Similar behavior has been reported for Ru^{II} and Re^{I}

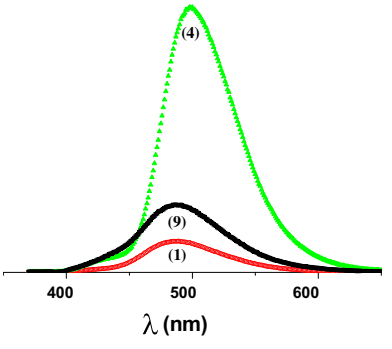

Figure 3. Comparison of the emission spectra of the symmetric Zn^{II} complexes with ethylenediamine (**1**) (○ red), *o*-phenylenediamine (**4**) (▲ green), with that of the unsymmetric Zn^{II} complex derived from ethylenediamine and *o*-phenylenediamine (**9**) (■ black) (see http://dx.doi.org/10.1080/00958972.2014.968145 for color version).

complexes [43, 44]. Excitation spectra of the complexes show the same behavior as the absorption spectra, proving that the ligand is responsible for the emission.

3.3. *Optical properties of the lamellar composites*

The energy gap for $MnPS_3$ was calculated from the solid state reflectance spectrum; a value of 2.5 eV was obtained (figure 4). However, the previously reported energy gap for this same layered phase by Kamata *et al.*, using photoelectron measurements, was 3.0 eV [45]. To explain the nature of this energy gap, the electronic structure of the thiophosphates was calculated in the eighties by Khumalo and Hughes [46]. The calculations showed that the valence band is constituted by the $3p_xp_y$ and 3s orbitals of the P–S bond, and the $3p_z$ orbital from the P–P bond, of P_2S_6 anion. The metal t_{2g} and e_g localized orbitals were obtained at higher energies as compared with the valence band. The conduction band at higher energy corresponds to the antibonding $3p_z$ of the P–P bond and sulfur [46]. According to Grasso, the main absorption band at 2.5 eV is from the valence band formed by the $3p_xp_y$ and 3s orbitals of the P–S bond to the atomic orbitals of the manganese ion [47–49].

As shown in table 3, all composites have spectra with energy gaps lower than the pristine $MnPS_3$ phase (2.5 eV). This can be explained by accepting that during the intercalation process the complexes lose their axial ligands and enter the interlamellar space as square planar cationic species [28]. This can be inferred from the interlamellar distance of 9.9 Å given by the powder diffraction data (figure 5) and the calculated distances for the macrocyclic species (height, ~14 Å; width, ~13 Å) (scheme 4). However, inside the interlamellar space the complexes are parallel to the layers and the metal centers interact with the protruding sulfurs, thus restoring their initial pyramidal square base geometry. In this way, the interaction of the metal centers and the ligands of the complexes may be assumed to be maximum with the inorganic network.

The optical data obtained from the reflectance spectra indicate that those composites with aliphatic amines still produce the shift of the energy gap, indicating that the shift in the energy value is not only due to delocalization in the macrocyclic ligand derived from the aromatic diamine (table 3). Thus, the importance of the interaction of the ligand with

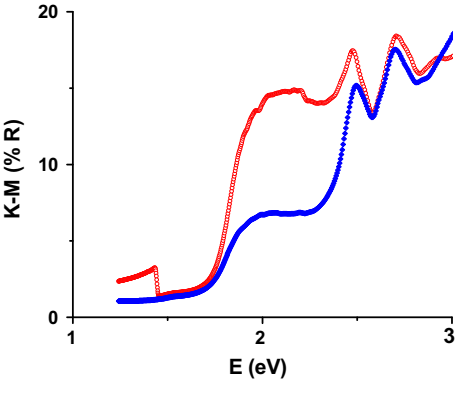

Figure 4. Diffuse reflectance spectra of composites $[Cu_2L^1]_{0.07}K_{0.26}Mn_{0.8}PS_3$ ***(a)*** (○ red) and $[Zn_2L^1]_{0.07}K_{0.26}Mn_{0.8}PS_3$ ***(e)*** (♦ blue) (see http://dx.doi.org/10.1080/00958972.2014.968145 for color version).

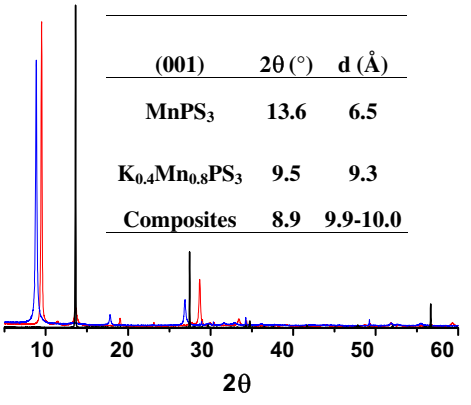

Figure 5. Diffractograms of the pristine phase $MnPS_3$ (black), the potassium precursor $K_{0.4}Mn_{0.8}PS_3$ (red), and a representative final composite $[Cu_2L^1]_{0.07}K_{0.26}Mn_{0.8}PS_3$ (blue) (see http://dx.doi.org/10.1080/00958972.2014.968145 for color version).

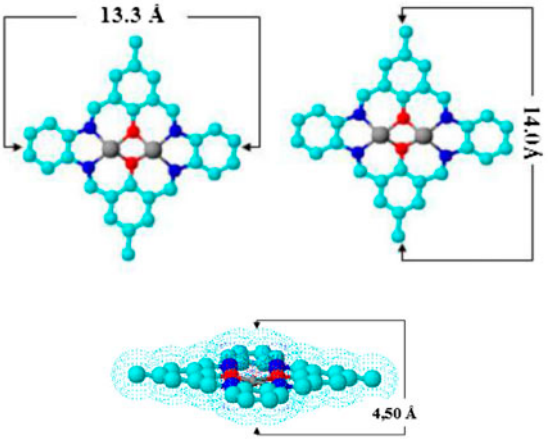

Scheme 4. Schematic representation of the intercalated complexes showing the main dimensions.

Table 3. Energy gap (eV) for the composites, derived from the intercalation of different macrocyclic complexes in MnPS3.

Composite	Energy gap (eV)	Energy gap (nm)
$[Cu_2L^1]_{0.07}K_{0.26}Mn_{0.8}PS_3$ ***(a)***	1.71	725
$[Cu_2L^3]_{0.07}K_{0.26}Mn_{0.8}PS_3$ ***(b)***	1.73	717
$[Cu_2L^5]_{0.08}K_{0.24}Mn_{0.8}PS_3$ ***(c)***	1.69	733
$[Cu_2L^7]_{0.09}K_{0.22}Mn_{0.8}PS_3$ ***(d)***	1.71	725
$[Zn_2L^1]_{0.07}K_{0.26}Mn_{0.8}PS_3$ ***(e)***	1.67	742
$[Zn_2L^4]_{0.12}K_{0.16}Mn_{0.8}PS_3$ ***(f)***	1.76	704
$[Zn_2L^4]_{0.05}K_{0.30}Mn_{0.8}PS_3]$ ***(3)****	1.85	670
$[Zn_2L^4]_{0.10}K_{0.20}Mn_{0.8}PS_3]$ ***(2)****	1.80	688

*Ref. [28].

the P–S of the P_2S_6 anions is still to be considered. However, the fact that the nature of the metal center does produce some small differences in the values of the energy gap of the composites can be considered as evidence that the interaction of the sulfur of the P_2S_6 anions with the metal centers of the intercalated complexes (Zn^{II}, Cu^{II}) also influences the obtained values of the absorption edge. Since the optical properties of composites of the same stoichiometry have to be compared [50], it is possible to give as an example $[Cu_2L^1]_{0.07}K_{0.26}Mn_{0.8}PS_3$ ***(a)*** and $[Zn_2L^1]_{0.07}K_{0.26}Mn_{0.8}PS_3$ ***(e)***, with $E_g = 1.71$ eV and $E_g = 1.67$ eV, respectively (figure 4). The above-mentioned observations indicate that the intercalated complexes have to be considered as a whole in their interaction with the protruding sulfurs of the lamellae, influencing the optical properties of the composites.

4. Conclusion

The spectroscopic properties of symmetric and unsymmetric macrocyclic Zn^{II} and Cu^{II} complexes suggest the importance of the nature of both the ligand and the metal center, on the absorption and emission behavior.

Due to the lower aromaticity of the unsymmetric ligands, the MLCT band is blue-shifted in spectra of the corresponding complexes, as compared with the symmetric complexes derived from *o*-phenylenediamine. For symmetric species, the intra-ligand bands in the spectra of the complexes with 1,3-diaminepropane and 1,3-diamine-2-propanol are blue-shifted as compared with spectra of the corresponding complexes with the macrocycle derived from ethylenediamine.

The emission band for the symmetric complexes with the aromatic ligand, derived from *o*-phenylenediamine, is red-shifted compared to those complexes which are based on macrocyclic ligands with ethylenediamine, 1,3-diaminopropane, and 1,3-diamino-2-propanol. The presence of the ligand derived from *o*-phenylenediamine enhances the emission of the complexes; the Zn^{II} complex (**4**) has the highest quantum yield, as compared with **1**, **2**, and **3**.

The unsymmetric macrocyclic Zn^{II} and Cu^{II} complexes emit between the emission wavelength of the corresponding symmetric complex with the aliphatic amine and the symmetric complex with *o*-phenylenediamine.

All composites have spectra with energy gaps lower than the pristine $MnPS_3$ phase (2.5 eV). Thus, the interaction of the intercalated complex in the interlamellar space influences the optical properties of the composites by decreasing the absorption edge of the corresponding spectra.

Acknowledgements

The authors thank FONDECYT project 1120001 and the LIA-MIF 836 international collaboration project (CNRS/CONICYT) for financial support. PFC acknowledges CONICYT doctoral grant and thesis support grant (21110612).

References

[1] I. Lagadic, P.G. Lacroix, R. Clément. *Chem. Mater.*, **9**, 2004 (1997).
[2] X. Zhang, H. Zhou, X. Su, X. Chen, C. Yang, J. Qin, M. Inokuchi. *J. Alloys Compd.*, **432**, 247 (2007).

[3] D. Zhang, J. Qin, K. Yakushi, Y. Nakazawa, K. Ichimura. *Mater. Sci. Eng., A*, **286**, 183 (2000).
[4] A. Murugan. *Electrochim. Acta*, **50**, 4627 (2005).
[5] L. Silipigni, G. Di Marco, G. Salvato, V. Grasso. *Appl. Surf. Sci.*, **252**, 1998 (2005).
[6] R. Clement, A. Leaustic, K. Marney, A.H. Francis. *J. Lumin.*, **60–61**, 355 (1994).
[7] D. Ruiz-León, V. Manríquez, J. Kasaneva, R.E. Avila. *Mater. Res. Bull.*, **37**, 981 (2002).
[8] X. Zhang, X. Su, X. Chen, J. Qin, M. Inokuchi. *Microporous Mesoporous Mater.*, **108**, 95 (2008).
[9] B.M. Choudary, S. Madhi, N.S. Chowdari, M.L. Kantam, B. Sreedhar. *J. Am. Chem. Soc.*, **124**, 14127 (2002).
[10] Y.V. Kuzminskii, B.M. Voronin, N.N. Redin. *J. Power Sources*, **55**, 133 (1995).
[11] P.G. Lacroix, R. Clement, K. Nakatani, J. Zyss. *Science*, **263**, 558 (1994).
[12] G. Abellán, F. Busolo, E. Coronado, C. Martí-Gastaldo, A. Ribera. *J. Phys. Chem. C*, **116**, 15756 (2012).
[13] E. Coronado, C. Martí-Gastaldo, E. Navarro-Moratalla, A. Ribera, J.R. Galán-Mascarós. *J. Mater. Chem.*, **20**, 9476 (2010).
[14] E. Coronado, J.R. Galán-Mascarós, C. Martí-Gastaldo, A. Ribera. *Chem. Mater.*, **18**, 6112 (2006).
[15] F.R. Gamble, F. DiSalvo, R. Klemm, T. Geballe. *Science*, **168**, 568 (1970).
[16] E. Coronado, C. Martí-Gastaldo, E. Navarro-Moratalla, E. Burzurí, A. Camón, F. Luis. *Adv. Mater.*, **23**, 5021 (2011).
[17] Y. Wu, H. Li, L. Ji, Y. Ye, J. Chen, H. Zhou. *Surf. Coat. Technol.*, **236**, 438 (2013).
[18] C.N.R. Rao, H.S.S. Ramakrishna Matte, U. Maitra. *Angew. Chem. Int. Ed.*, **52**, 13162 (2013).
[19] Q. Liu, W. Zhou, Ch Gao, T. Hu, X. Zhao. *Chem. Phys. Lett.*, **477**, 388 (2009).
[20] N. Ismail, M. Madian, A.A. El-Meligi. *J. Alloys Compd.*, **588**, 573 (2014).
[21] A.A. El-Meligi, A.M. Al-Saie, H. Al-Buflasa, M. Bououdina. *J. Alloys Compd.*, **488**, 284 (2009).
[22] S. Floquet, S. Salunke, M.L. Boillot, R. Clément, F. Varret, K. Boukheddaden, E. Rivière. *Chem. Mater.*, **14**, 4164 (2002).
[23] E. Spodine, P. Valencia-Gálvez, P. Fuentealba, J. Manzur, D. Ruiz, D. Venegas-Yazigi, V. Paredes-García, R. Cardoso-Gil, W. Schnelle, R. Kniep. *J. Solid State Chem.*, **184**, 1129 (2011).
[24] P. Zanello, S. Tamburini, P.A. Vigato, G.A. Mazzocchin. *Coord. Chem. Rev.*, **77**, 165 (1987).
[25] X. Zhang, H. Zhou, X. Su, X. Chen, Ch Yang, J. Qin, M. Inokuchi. *J. Alloys Compd.*, **432**, 247 (2007).
[26] H. Ōkawa, H. Furutachi, D.E. Fenton. *Coord. Chem. Rev.*, **174**, 51 (1998).
[27] M. Mukhopadhyay, D. Banerjee, S. Mukherjee. *J. Phys. Chem. A*, **110**, 12743 (2006).
[28] E. Spodine, P. Valencia-Gálvez, J. Manzur, V. Paredes-García, N. Pizarro, K. Bernot, D. Venegas-Yazigi. *Polyhedron*, **44**, 187 (2012).
[29] D. Venegas-Yazigi, D. Aravena, E. Spodine, E. Ruiz, S. Alvarez. *Coord. Chem. Rev.*, **254**, 2086 (2010).
[30] G.A. Crosby, J.N. Demas. *J. Phys. Chem.*, **75**, 991 (1971).
[31] E.P. Papadopoulos, A. Jarrar, C.H. Issidorides. *J. Org. Chem.*, **31**, 615 (1966).
[32] V. Paredes-García, D. Venegas-Yazigi, A. Cabrera, P. Valencia, M. Arriagada, D. Ruiz-León, N. Pizarro, A. Zanocco, E. Spodine. *Polyhedron*, **28**, 2325 (2009).
[33] S. Sreedaran, K. Bharathi, A. Rahiman, K. Rajesh, G. Nirmala, L. Jagadish, V. Kaviyarasan, V. Narayanan. *Polyhedron*, **27**, 1867 (2008).
[34] S.K. Dutta, U. Flörke, S. Mohanta, K. Nag. *Inorg. Chem.*, **37**, 5029 (1998).
[35] L.K. Thompson, S.K. Mandal, S.S. Tandon, J.N. Bridson, M.K. Park. *Inorg. Chem.*, **35**, 3117 (1996).
[36] S.S. Tandon, L.K. Thompson, J.N. Bridson, V. McKee, A.J. Downard. *Inorg. Chem.*, **31**, 4635 (1992).
[37] D. Venegas-Yazigi, S. Cortés, V. Paredes-García, O. Peña, A. Ibañez, R. Baggio, E. Spodine. *Polyhedron*, **25**, 2072 (2006).
[38] E. Spodine, Y. Moreno, M.T. Garland, O. Pena, R. Baggio. *Inorg. Chim Acta*, **309**, 57 (2000).
[39] K. Brychcy, K. Dräger, K.-J. Jens, M. Tilset, U. Behrens. *Chem. Ber.*, **127**, 465 (1994).
[40] S.R. Korupoju, N. Mangayarkarasi, S. Ameerunisha, E.J. Valente, P.S. Zacharias. *J. Chem. Soc., Dalton Trans.*, 2845 (2000).
[41] D.N. Kumar, B.S. Garg. *Spectrochim. Acta, Part A*, **64**, 141 (2006).
[42] ThM Rajendiran, R. Kannappan, R. Mahalakshmy, J. Rajeswari, R. Venkatesan, P. Rao. *Transition Met. Chem.*, **28**, 447 (2003).
[43] A.P. Zipp, L. Sacksteder, J. Streich, A. Cook, J.N. Demas, B.A. DeGraff. *Inorg. Chem.*, **32**, 5629 (1993).
[44] R.H. Schmehl, I.V. Rubtsov, T.A. Grusenmeyer, Y. Yue, J. Pham. *Abstr. Pap. Am. Chem. Soc.*, **245** (2013).
[45] A. Kamata, K. Noguchi, H. Tezuka, T. Kashiwakura, Y. Ohno, Sh. Nakai. *Phys. Soc. Jpn.*, **66**, 401 (1997).
[46] F.S. Khumalo, H.P. Hughes. *Phys. Rev. B*, **23**, 5375 (1981).
[47] V. Grasso, S. Santangelo, M. Piacentini. *Solid State Ionics*, **20**, 9 (1986).
[48] V. Grasso, F. Neri, L. Silipigni. *Il Nuovo Cimento*, **13**, 633 (1991).
[49] V. Grasso, F. Neri, S. Santangelo, L. Silipigni, M. Piacentini. *J. Phys. Condens. Matter*, **1**, 3337 (1989).
[50] P. Valencia, J. Manzur, A.M. Garcia, V. Paredes-Garcia, R. Cardoso-Gil, W. Schnelle, R. Kniep, P. Fuentealba, D. Venegas-Yazigi, E. Spodine. *J. Chil. Chem. Soc.*, **58**, 1952 (2013).